

BIROn - Birkbeck Institutional Research Online

Jordan, S.F. and Rammu, H. and Zheludev, I.N. and Hartley, Andrew and Marechal, Amandine and Lane, N. (2019) Promotion of protocell self-assembly from mixed amphiphiles at the origin of life. *Nature Ecology & Evolution* , ISSN 2397-334X.

Downloaded from: <https://eprints.bbk.ac.uk/id/eprint/29841/>

Usage Guidelines:

Please refer to usage guidelines at <https://eprints.bbk.ac.uk/policies.html> or alternatively contact lib-eprints@bbk.ac.uk.

1 **Promotion of protocell self-assembly from mixed amphiphiles at the origin of life**

2

3 Sean F. Jordan¹, Hanadi Rammu¹, Ivan N. Zheludev¹, Andrew M. Hartley², Amandine Maréchal^{2,3},

4 Nick Lane¹

5

6 ¹*Centre for Life's Origin and Evolution, Department of Genetics, Evolution and Environment, Darwin*

7 *Building, Gower Street, University College London, London WC1E 6BT, UK*

8 ²*Institute of Structural and Molecular Biology, Birkbeck College, London, WC1E 7HX, UK*

9 ³*Institute of Structural and Molecular Biology, University College London, London, WC1E 6BT, UK*

10

11 **Corresponding author:** Nick Lane nick.lane@ucl.ac.uk

12

13 **Key words:** origin of life, protocells, single-chain amphiphiles, fatty acids, 1-alkanols, vesicles,

14 alkaline hydrothermal vents, self-assembly

15

16 **Abstract**

17

18 Vesicles formed from single-chain amphiphiles (SCAs) such as fatty acids likely played an important

19 role in the origin of life. A major criticism of the hypothesis that life arose in an early ocean

20 hydrothermal environment is that hot temperatures, large pH gradients, high salinity and abundant

21 divalent cations should preclude vesicle formation. But these arguments are based on model vesicles

22 using 1-3 SCAs, even though Fischer-Tropsch-type synthesis under hydrothermal conditions

23 produces a wide array of fatty acids and 1-alkanols, including abundant C₁₀-C₁₅ compounds. Here we

24 show that mixtures of these C₁₀-C₁₅ SCAs form vesicles in aqueous solutions between pH ~6.5 to >12

25 at modern seawater concentrations of NaCl, Mg²⁺ and Ca²⁺. Adding C₁₀ isoprenoids improves vesicle

26 stability even further. Vesicles form most readily at temperatures of ~70 °C and require salinity and

27 strongly alkaline conditions to self-assemble. Thus, alkaline hydrothermal conditions not only permit
28 protocell formation at the origin of life but actively favour it.

29

30 **Introduction**

31

32 Membranes are fundamental to life, the nexus between cell and environment. Peter Mitchell wrote
33 “I cannot consider the organism without its environment... from a formal point of view the two may
34 be regarded as equivalent phases between which dynamic contact is maintained by the membranes
35 that separate and link them”¹. Beyond the requirement for compartmentalisation, differences in ion
36 concentration across the plasma membrane drive CO₂ fixation and energy metabolism in all modern
37 autotrophic cells by vectorial chemistry²⁻⁴. This deep conservation of membrane bioenergetics also
38 points to the fundamental role of membranes at the origin of life²⁻⁴.

39 Despite their clear importance across life, the composition of early membranes is uncertain.
40 The universality of membrane proteins with equivalent transmembrane helices indicates that early
41 cells had some sort of lipid bilayer⁵. But the phospholipid membranes of bacteria and archaea differ
42 in their chemistry, most strikingly in the stereochemistry of their glycerol phosphate headgroups –
43 archaea typically have glycerol-1-phosphate while bacteria have glycerol-3-phosphate⁶⁻⁸. There is no
44 known selective basis for this distinction⁹, suggesting that their common ancestor did not possess a
45 modern phospholipid membrane but instead had a simpler bilayer composed largely of single-chain
46 amphiphiles (SCAs), perhaps including fatty acids and isoprenoids (which are found in both bacteria
47 and archaea¹⁰, and are perfectly compatible membrane components^{11,12}). SCAs can assemble to
48 form droplets, micelles or lipid bilayers in aqueous solutions depending on pH (Extended Data Fig.
49 1). Bilayer membranes composed of SCAs facilitate simple growth, being able to incorporate new
50 lipids directly¹³⁻¹⁵. In principle, proton-permeable SCA membranes are also required for cells to
51 harness geological ion gradients without collapsing to equilibrium, potentially shedding light on the
52 deep divergence between bacteria and archaea^{4,16}.

53 The idea that the first cell membranes were composed of SCAs is appealing from the
54 standpoint of prebiotic chemistry^{17,18}. Fatty-acid synthesis is thermodynamically favoured under mild
55 hydrothermal conditions (25-150 °C) at alkaline pH¹⁹. Lipids have been synthesised from formate via
56 Fischer-Tropsch-type reactions under hydrothermal conditions (100-150 °C), albeit in steel reactors,
57 suggesting that iron (or carbon-metal bonds²⁰) might be a critical electron donor or catalyst²¹. The
58 lipids formed include abundant long-chain fatty acids and 1-alkanols (mainly C₆-C₁₆)²¹. Likewise, the
59 reaction of acetylene (C₂H₂) and CO in contact with nickel sulfide (NiS) in hot aqueous medium at pH
60 7-9 can form long-chain (up to C₉) unsaturated monocarboxylic acids²². Branched-chain pentoses
61 containing the isoprene skeleton are formed under mild alkaline hydrothermal conditions (60-90 °C,
62 pH 9-11) via the formose reaction²³. Higher pressure in submarine hydrothermal vents should favour
63 synthesis of longer-chain amphiphiles, according to Le Chatelier's principle²¹, as well as greatly
64 increasing hydrogen solubility²⁴. Thermophoresis in porous hydrothermal systems can concentrate
65 amphiphiles above the critical bilayer concentration to form vesicles spontaneously^{25,26}. Mineral
66 surfaces including silicates and FeS minerals found in hydrothermal systems can also enhance vesicle
67 assembly²⁷. Theoretical modelling suggests that vectorial CO₂ reduction on FeS clusters associated
68 with protocell membranes (which are homologous to the proton-motive Energy-converting
69 hydrogenase in methanogens²⁸) could drive protocellular growth and establish a rudimentary form
70 of membrane heredity²⁹. All these factors point to alkaline hydrothermal systems as prebiotic
71 electrochemical reactors^{4,7,30-35} capable of driving the synthesis of amphiphiles, and then
72 concentrating them *in situ*, to form protocells at the origin of life.

73 But there is also a potentially serious drawback. One of the major criticisms of alkaline
74 hydrothermal vents as a setting for the origin of life is that the relatively harsh environment is not
75 conducive to the formation of vesicles³⁶⁻³⁹. Specifically, previous laboratory work has shown that
76 strongly alkaline pH, high temperatures, ocean salinity and abundant divalent cations all disrupt the
77 formation of vesicles from SCAs³⁶⁻⁴⁰. The conclusion that amphiphilic compounds 'do not assemble
78 into vesicles in seawater' might seem fatal to the idea that life originated in deep-sea hydrothermal

79 vents⁴⁰. Yet this conclusion is based on vesicles composed of decanoic acid or simple mixtures of two
80 or three amphiphiles. Mixtures of SCAs with more complex head groups (such as amine, glycerol,
81 and sulfate) have been shown to form vesicles over a wider pH range, albeit predominantly at
82 neutral and acidic pH^{41,42}. The addition of 1-alkanols can stabilize fatty-acid vesicles at the high pH
83 found in alkaline vents^{43,44}. Vesicles composed of decylamine and decanoic acid are stable even at
84 pH 11 in the presence of some salts, but they produce curious crystalline aggregates between pH 2
85 and 10, while their prebiotic provenance is uncertain⁴⁵. Polyaromatic hydrocarbons (PAH) seem to
86 improve vesicle stability further, although they have little congruence with modern membranes^{45,46}.
87 Yet despite these various indications that mixtures of amphiphiles can enhance vesicle stability, the
88 combination of strongly alkaline pH, high temperatures, high salinity and abundant divalent cations
89 is still often cited as an insuperable barrier to life beginning in oceanic hydrothermal systems³⁶⁻⁴⁰.
90 We have therefore explored the properties of vesicles assembled from mixtures of the 6-12 most
91 abundant SCAs formed through hydrothermal Fischer-Tropsch-type synthesis²¹, combined with two
92 simple isoprenoid molecules. Far from precluding vesicle formation at the origin of life, we show
93 that alkaline hydrothermal conditions in fact promote vesicle assembly from these prebiotically
94 plausible mixtures of amphiphiles.

95

96 **Results**

97 A 50 mM solution of pure decanoic acid vesicles (one of the most widely investigated vesicle forming
98 SCAs in origin of life research) was first tested to ensure that the methods employed here yielded
99 results matching literature values. These results provided a transition point of pH ~7.2 and a range of
100 vesicle formation of ~0.2 pH units, which is similar to previously reported values (Fig. 1)⁴⁷. The first
101 complex solution of vesicles that we investigated was a mixture of fatty acids from C₁₀ to C₁₅
102 including both odd and even chain-lengths (all of which are formed by Fischer-Tropsch-type
103 synthesis under hydrothermal conditions) giving a total of six SCAs. A concentration of 5 mM (of
104 each SCA) was used to test vesicle stability across a pH range of ~7 to 13. When fitted to a sigmoid

curve (see Supplementary Information) a transition point of pH ~ 8.45 was observed (Fig. 1). Confocal microscopy of the solution at this pH value confirmed the presence of vesicles (Fig. 1). A greater abundance of vesicles was observed at pH values below these transition points (Supplementary Figs. 1 and 2). The transition point appears to be a conservative estimate of the initiation point of vesicle formation, as confocal microscopy shows the presence of vesicles in mixed fatty acid solutions as high as pH ~ 9 whereas the observed transition point is pH ~ 8.5 (Supplementary Fig. 3).

Solutions containing fatty acids and 1-alkanols were prepared in molar ratios of 10:1, 5:1, and 1:1. The pH range of vesicle formation was unaffected by the addition of 1-alkanols in a 10:1 ratio, giving a transition point of pH ~ 8.5 , similar to that of fatty acids alone (Extended Data Fig. 2). But with a 5:1 ratio, the range was extended to a transition point of pH ~ 9.5 (Fig. 1). For a solution containing a 1:1 ratio of fatty acids to 1-alkanols vesicle formation was observed from pH ~ 6.5 to 13 with no obvious transition point (Fig. 2a). Confocal microscopy confirms the presence of vesicles in solution across the entire pH range (Fig. 2). Encapsulation of the fluorescent dye pyranine clearly shows that these vesicles can trap and retain the dye (Fig. 3a) for periods of at least 24 h at pH 12 (Fig. 3b) confirming that they have an aqueous lumen and are stable over hours to days. Note that the fluorescence associated with vesicles after 24 h had fallen to 15-20% that of fresh vesicles.

The CBC of the mixed fatty acid solution was determined to be 1.3 mM by OD measurements (Fig. 4), with each SCA at a concentration of 225 μM . However, confocal microscopy at concentrations below 6 mM (combined SCA) did not reveal any vesicles in these solutions. We hypothesised that at lower concentrations, vesicles are smaller in size than those at higher concentrations. To test this, cryo-TEM analysis was conducted on mixed fatty acid solutions below 6 mM concentration (with individual SCA concentrations of 100, 200, 300, 400, and 500 μM). These results showed that vesicles did in fact form in solutions as low as 600 μM total concentration but they were less than 200 nm in diameter, lower than the resolution limit of the confocal microscope (Fig. 4). These tiny vesicles do appear to have bounding membranes on cryo-TEM, although their appearance is equivocal, and it is possible that they are lipid droplets. Nonetheless, NS-TEM shows

unequivocal evidence of the collapsed doughnut shapes associated with vesicles, on an equivalent scale (Extended Data Figs. 3 and 4). We therefore think it most likely that low concentrations of SCAs do simply produce smaller vesicles. These small vesicles were present in higher concentration solutions as well and are likely present at most concentrations tested but are simply not observable under a confocal microscope. If so, then the CBC determined by the OD analysis is a conservative estimate of the minimum SCA concentration required for vesicle formation, as OD measurements are diffraction-limited in the same way as confocal microscopy. CBC values for the 5:1 and 1:1 solutions were similar to those of fatty acids alone, and vesicles likely form below this concentration in these solutions as well (Extended Data Fig. 5).

Due to the extremely wide pH range of vesicle formation observed for 5 mM 1:1 solutions, this model was selected for further testing under the influence of salinity and divalent cations. Solutions were prepared in a range of conditions and analysed by confocal microscopy, cryo-TEM, NS-TEM and pyranine encapsulation. Modern day seawater contains on average 600 mM NaCl, 50 mM Mg^{2+} , and 10 mM Ca^{2+} . These values are frequently cited as precluding the assembly of SCA vesicles, excluding any oceanic environment as a potential location for the origin of life^{39,40}. As such, these concentrations were employed as the maximum concentrations for our experiments on the effects of salinity and divalent cations on vesicle formation, up to an ionic strength in the full salt mix of 1.022 M (Supplementary Table 1). Vesicles were prepared in a range of 100 – 600 mM NaCl at pH ~9 and 12 and were observed in all solutions at pH ~12 (Fig. 5, Extended Data Fig. 6 and Supplementary Fig. 4). Vesicles were prepared from 10 – 50 mM $MgCl_2$ and 1 – 10 mM $CaCl_2$ at pH ~7, 9, and 12. Again, vesicle formation was observed at all concentrations at pH ~12 (Fig. 5, Extended Data Figs. 7 and 8 and Supplementary Figs. 5 and 6) but no vesicles were observed at pH 7 or 9 in the presence of 20 mM $MgCl_2$ or 5 mM $CaCl_2$ (Supplementary Fig. 7), so we did not test higher concentrations. Vesicles were formed at lower concentrations of salt and divalent cations below pH 12. Vesicles could also form long filaments, seen by both confocal microscopy and NS-TEM. While their structure was unclear by confocal microscopy, the filaments appeared to be composed of

chains of individual vesicles by NS-TEM (Fig. 6). Note that vesicles burst under vacuum and so appear collapsed during microscopy.

Finally, 5 mM 1:1 fatty acid:1-alkanol vesicles were prepared in an alkaline (pH >12) solution containing a combination of NaCl, Mg^{2+} , and Ca^{2+} at modern seawater concentrations, thereby providing a more realistic analogue environment. Under these conditions, individual vesicles were not formed, and aggregates of vesicles were the predominant structures seen. It should be noted that cooling of vesicle solutions has been shown to lead to aggregation⁴⁰. As the microscope stage used here was not heated, cooling of the solutions from their original 70 °C temperature may also have contributed to this aggregation. This experiment was repeated with the addition of equimolar amounts of two C_{10} isoprenoids, geranic acid and geraniol, which are prebiotically plausible molecules that are significantly under-researched in terms of their potential for prebiotic vesicle formation. The inclusion of these two compounds enabled the formation of vesicles in an alkaline solution (pH 12) containing a combination of 600 mM NaCl, 50 mM Mg^{2+} , and 10 mM Ca^{2+} observed by confocal microscopy and cryo-TEM (Fig. 7) and confirmed by NS-TEM (Extended Data Fig. 9 and Supplementary Figs. 8-10).

To demonstrate that the vesicles observed independently by several different types of microscopy are indeed stable vesicles with a lumen, we examined their encapsulation of pyranine. Fig. 3c shows that vesicles composed of the full amphiphile mix can encapsulate pyranine in water, while Fig. 3d shows that the dye is retained over at least 24 h, demonstrating the stability of these vesicles. However, encapsulation experiments are more problematic under high salt conditions, especially in the presence of divalent cations, as most dyes, including the standards normally used for vesicle work, pyranine and calcein, interact with divalent cations or precipitate as hydroxides^{48,49} (Supplementary Fig. 11). Control preparations of pyranine in water with or without salts (i.e. with no SCAs present) show that pyranine fluorescence is largely suppressed in the presence of salts (Fig. 3e). Despite these issues, by preparing vesicles in the presence of pyranine, and adding a double-concentration salt mixture to achieve the required total salt concentration after encapsulation, we

were able to demonstrate that 1:1:1 mixtures of all SCAs can indeed form stable vesicles capable of encapsulating the dye in alkaline solution (pH 12) containing a combination of 600 mM NaCl, 50 mM Mg^{2+} , and 10 mM Ca^{2+} (Fig. 3f). We note these vesicles are able to retain the dye despite the osmotic shock of being added to double-strength full-salt mixtures. We also achieved encapsulation with calcein, despite interactions with salts (Extended Data Fig. 10). These findings confirm the cryo-TEM, confocal microscopy and NS-TEM demonstrating that vesicles are indeed formed under oceanic alkaline hydrothermal conditions.

Discussion

Our results show that mixtures of 6-14 SCAs, including fatty acids, 1-alkanols and isoprenoids, can form stable vesicles in aqueous solution across a pH range of ~6 units from pH ~6.5 to >12. We have demonstrated vesicle stability under these conditions by encapsulation of the fluorescent dye pyranine over 24 h (Fig. 3) and shown the presence of vesicles by multiple methodologically wholly distinct techniques, including cryo-TEM, NS-TEM, confocal microscopy, UV-Vis and fluorescence spectroscopy. Warm (70 °C), alkaline (pH 12) solutions equivalent to those found in modern alkaline hydrothermal vents^{34,50,51} actively promote vesicle formation and mitigate the interference produced by high concentrations of NaCl, Mg^{2+} , and Ca^{2+} . In Hadean deep-ocean alkaline hydrothermal systems, vesicles should have formed readily from mixtures of prebiotic SCAs, likely produced by Fischer-Tropsch-type synthesis²¹, giving rise to protocells at the origin of life.

Hydrothermal Fischer-Tropsch-type synthesis has been shown to form complex mixtures of fatty acids and 1-alkanols, as well as long-chain alkanes and alkenes, which decrease in their abundance with chain lengths above ~15 carbons²¹. We therefore used mixtures of these SCAs with chain-lengths from C_{10} - C_{15} . Compared with the C_{10} decanoic acid, longer chain lengths lower the critical bilayer concentration (CBC) by promoting more interactions between hydrophobic tails^{52,53}, effectively decreasing fatty acid solubility. Mixtures of fatty acids and 1-alkanols decrease the CBC still further, presumably through hydrogen bonding between the carboxylate and alcohol

headgroups^{37,38,41,54}. Vesicles assembled from decanoic acid alone have a CBC of 39 mM, whereas mixtures of 12 C₁₀-C₁₅ fatty acids and 1-alkanols (1:1) have a CBC around 30-fold lower, at 1.3 mM with a concentration of 225 μ M for each individual SCA. In fact, we found plentiful very small (<200 nm diameter) vesicles by NS-TEM and cryo-TEM at even lower concentrations (100 μ M for each SCA; Fig. 4). In vents, a combination of hydrothermal Fischer-Tropsch-type synthesis (producing complex mixtures of SCAs with low CBCs²¹) with thermophoresis (concentrating SCAs above the CBC via thermal currents^{25,26}) and interactions with mineral surfaces (enhancing vesicle assembly²⁷) should promote vesicle formation even at very low SCA concentrations.

More complex SCA mixtures dramatically increase vesicle assembly under strongly alkaline conditions. Raising the number of fatty acids in solution from one to six expands the pH range of vesicle formation nearly 100-fold, from about 0.2 to almost 2 pH units (Fig. 1). Increasing the content of 1-alkanols elicits an even greater effect. In 1:1 mixtures with fatty acids, 1-alkanols produce stable vesicles above pH 12, as seen from the OD data, confocal images (Fig. 2) and encapsulation of the fluorescent dye pyranine over 24 h (Fig. 3). Vesicles form when amphiphiles are in solution at a pH close to their pK_a, meaning they exist in both their protonated and deprotonated forms⁵⁵. Hydrogen bonding between protonated and deprotonated headgroups stabilizes bilayer structures. In contrast, protonation under acidic conditions promotes the formation of droplets, whereas deprotonation in alkaline conditions dissolves fatty acids or promotes micelle formation. Under alkaline hydrothermal conditions, fatty acids are well above their pK_a, hence all carboxylic acid headgroups deprotonate, favouring dissolution⁴⁷. Lengthening the fatty-acid chains raises the apparent pK_a through hydrophobic interactions between their tails^{52,53}, but this effect is limited. Adding 1-alkanols strongly promotes vesicle formation as the alcohol headgroups do not deprotonate^{37,55}. A 1:1 mixture of fatty acids and 1-alkanols therefore forms vesicles at high pH as the headgroups of the two species are equally protonated and deprotonated, forming stable hydrogen bonds even in strongly alkaline conditions (Fig. 2).

The standard lab procedure to promote vesicle self-assembly begins with deprotonated fatty acids at high pH, to ensure that amphiphiles are in solution or micellar form⁴⁷. The pH is then titrated down to the apparent pKa, whereupon vesicles self-assemble. In other words, vesicles do not form spontaneously at lower pH, but initially require strongly alkaline pH to self-assemble. While it is possible to form vesicles without raising the pH, we note that this can be achieved only after adding NaOH in the presence of buffer. In the absence of buffers, alkaline conditions are necessary to first deprotonate and dissolve fatty acids. We have observed that simply adding SCAs to salty water at pH 7 does not form vesicles, as the fatty acids are mostly protonated and form an emulsion of lipid droplets rather than bilayer vesicles. Once deprotonated and dissolved under alkaline conditions, titration down to more acidic conditions, as in the lab procedure, now forms bilayer vesicles. This titration would occur naturally by mixing with mildly acidic ocean waters in Hadean vents⁵⁶, and does not disassemble vesicles except at pH below 6.5 (though earlier work shows that vesicles can also form even at strongly acidic pH^{42,45}). With more complex mixtures of fatty acids and 1-alkanols, there is no need to titrate with acid to form vesicles, as they form spontaneously even above pH 12, even in the absence of salts. Initial heating is needed for similar reasons. Vesicles do not form readily from solid fatty acids below their melting point (or when protonated, as noted above). The melting point of fatty acids and 1-alkanols depends on chain length, with C₁₅ fatty acids melting around 53 °C. To dissolve long-chain SCAs therefore requires temperatures similar to those found in alkaline hydrothermal vents (typically 50-90 °C)^{34,50,51}; we used 70 °C. Once formed at warm temperatures, vesicles are still present on cooling (Supplementary Fig. 12), again consistent with mixing in the vents with cooler ocean waters. Far from precluding protocell formation, the pH and temperature range in alkaline hydrothermal vents should therefore promote their self-assembly at the origin of life.

Salinity is also known to promote vesicle assembly through both polar (electrical shielding of the charged headgroups) and non-polar (more pronounced phase partitioning of hydrophobic tails) effects^{42,54}. Nonetheless, earlier work concluded that high salt concentrations (>150 mM) disrupt vesicle formation and would preclude the formation of protocells at modern ocean salinity (~600

mM NaCl)³⁷⁻⁴¹. If the salinity of Hadean oceans were equivalent, this reasoning goes, then life could not have begun in the oceans and must have started in terrestrial freshwater pools. The inferred salinity of Hadean oceans is difficult to constrain. Extrapolations based on fluid inclusions trapped in ancient rocks are questionable⁵⁷, but three factors are pertinent: (i) acid leaching of the crust by hot early oceans should have released Na⁺ into the oceans rapidly, so that maximum salinity was reached quickly⁵⁷; (ii) the lack of evaporitic salt deposits in the Hadean, given practically global oceans, means that Hadean oceans could have had nearly double the salt content of modern oceans⁵⁸; but (iii) the sequestration of water as hydrated minerals (e.g. serpentinites) over 4.5 billion years means that Hadean oceans could have had twice the volume of modern oceans⁵⁹⁻⁶¹. A conservative position is therefore that ocean salinity was similar to today. If life started in the oceans, then protocells would need to tolerate ~600 mM NaCl.

The difficulty of forming vesicles at modern ocean salinity reported by others can best be ascribed to the use of simple mixtures of largely C₁₀ SCAs. We show that more complex mixtures of 12 C₁₀-C₁₅ fatty acids and 1-alkanols do indeed form numerous individual vesicles at modern ocean salinity (Fig. 5). Higher salinity sometimes promotes the aggregation of vesicles or the formation of filamentous structures observed by confocal microscopy (Fig. 6) and certainly there are fewer individual vesicles under these conditions. However, NS-TEM analysis suggests that these filaments are composed entirely of individual SCA vesicles (Fig. 6). The vesicles burst under vacuum, so appear collapsed during microscopy. Similar structures have been found in liposome research previously (by both confocal microscopy and NS-TEM, as reported here) and are known to be metastable⁶²⁻⁶⁴. More work is needed to characterise these remarkable structures and elucidate their chemical properties in an origin-of-life context.

Divalent cations, notably Mg²⁺ and Ca²⁺, have also been shown to disrupt vesicle formation^{39,40}. Their concentration in Hadean oceans is unknown, and estimates vary greatly^{65,66}. Ocean levels are in any case a poor surrogate for vent systems; the concentration of Ca²⁺ and Mg²⁺ in modern alkaline vent fluids is extremely variable, with some features containing no Ca²⁺ or Mg²⁺ at

all⁶⁷. We therefore examined vesicle stability in the presence of modern seawater concentrations of Mg^{2+} and Ca^{2+} , as earlier work reported that seawater levels aggregate fatty acid/1-alkanol vesicles into insoluble curds^{39,40}. While simple organic chelators such as citrate can prevent this from happening⁶⁸ (and vesicles composed of decylamine and decanoic acid have been shown to form in the presence of 0.1 M Mg^{2+} and Ca^{2+} salts⁴⁴) we find that alkaline pH alone offers some protection. Divalent cations form complexes with amphiphile head groups at low pH, prohibiting bilayer formation and producing soapy solutions^{36-41,47,55}. In contrast, strongly alkaline conditions favour hydroxide complexes with these inorganic ions, in effect rendering them unavailable for vesicle disruption. Plentiful vesicles form at strongly alkaline pH (pH 11-12) in the presence of 50 mM Mg^{2+} and 10 mM Ca^{2+} (Fig. 5) but very few form at pH <9 (Supplementary Fig. 7). While the combination of modern seawater concentrations of NaCl, Mg^{2+} and Ca^{2+} at pH 11 and 70 °C did disrupt vesicle formation with mixtures of 12 C₁₀-C₁₅ fatty acids and 1-alkanols, addition of two C₁₀ isoprenoids, geranic acid and geraniol enabled vesicle assembly even under these most extreme conditions, as demonstrated by confocal microscopy, cryo-TEM (Fig. 7) and NS-TEM (Extended Data Fig. 9 and Supplementary Figs. 8-10). We confirmed the stability of these vesicles in oceanic alkaline hydrothermal conditions through encapsulation of the fluorescent dye pyranine (Fig. 3). We explore the reasons for this increased stability elsewhere⁶⁹.

We conclude that deep-sea alkaline hydrothermal conditions in the Hadean should have promoted the synthesis of long-chain amphiphiles and their self-assembly into protocells at the origin of life. Thermophoresis²⁶ and interactions with mineral surfaces in porous vents²⁷ concentrate amphiphiles above the critical bilayer concentration. Vents sustain the moderately high temperatures needed to ensure that longer chain amphiphiles are above their melting point and so available for vesicle formation in solution⁴¹. Alkaline pH is essential to dissolve the SCAs in water, deprotonating the head-groups of some amphiphiles and reducing the concentration of divalent cations such as Ca^{2+} and Mg^{2+} in solution. Titration by mixing with more acidic ocean waters within vents favours vesicle self-assembly. Salts promote vesicle assembly⁴¹ as well as aggregation of three-

dimensional structures that could potentially harness geologically sustained pH gradients to drive CO₂ fixation^{29,70,71}. Mixtures of amphiphiles are geochemically²¹ and biochemically⁷² meaningful, and are critical to forming protocells capable of growth and simple heredity²⁹ at the origin of life.

Methods

Materials

Decanoic acid, dodecanoic acid, tetradecanoic acid, decan-1-ol, undecan-1-ol and geraniol were purchased from Acros Organics. Undecanoic acid, tridecanoic acid, tridecan-1-ol, geranic acid, sodium chloride (NaCl), calcium chloride dihydrate (CaCl₂·2H₂O), Sephadex G-50 and 8-hydroxypyrene-1,3,6-trisulfonic acid (pyranine) were purchased from Sigma Aldrich. Pentadecanoic acid, dodecan-1-ol, tetradecan-1-ol, pentadecan-1-ol and magnesium chloride hexahydrate (MgCl₂·6H₂O) were purchased from Alfa Aesar. All reagents used were analytical grade (≥ 97%).

Preparation of vesicle solutions

All laboratory work was carried out in a dry heat block (SciQuip HP120-S) at 70 °C. Density values for each compound at this temperature were obtained gravimetrically (Supplementary Table 2). Vesicle solutions were prepared daily following a modified version of the procedure outlined by Monnard and Deamer⁴⁷. Buffers were not employed in any solutions in an effort to maintain prebiotic relevance. A 7 mL 10 mM stock solution of vesicles was prepared by adding equimolar concentrations of each fatty acid to 4 mL of deionised H₂O in a glass vial. The pH was adjusted to >12 with 500 µL 1 M NaOH and the solution was vortexed to ensure full dissolution of deprotonated acids. For vesicles containing 1-alkanols, equimolar concentrations were added at this stage and the solution was vortexed. The solution was then brought to a final volume of 7 mL with 1 M NaOH (final pH ~12). 500 µL of the stock solution was added to a fresh glass vial. The solution was titrated with gradual addition of 1 M HCl followed by pH measurement (Fisher Scientific accumet AE150 meter with VWR semi-micro pH electrode) to achieve the desired pH. The solution was brought to a final

volume of 1 mL with deionised H₂O resulting in a concentration of 5 mM after which the pH value was recorded. For isoprenoid-containing solutions, isoprenoid acids and alcohols were added in conjunction with fatty acids and 1-alkanols respectively.

For critical bilayer concentration (CBC) experiments, the same procedure was used followed by serial dilution in order to obtain the desired concentrations. The pH of each solution was measured again prior to analysis. In order to test the influence of NaCl, Mg²⁺, and Ca²⁺, this procedure was carried out using aqueous solutions of the desired salt concentration in the place of H₂O. Identical quantities of salts were dissolved in 1M NaOH and 1M HCl for use in pH adjustment, thereby ensuring that the concentration of salt remained constant throughout the experiment.

Determination of vesicle formation and CBC

Optical density (OD) measurements were obtained by measuring absorbance at 480 nm on an Infinite M200 Pro Spectrophotometer (Tecan) and data was processed using the Magellan software package. Three 50 µL aliquots of each solution were transferred to separate wells on a Falcon black 96 well plate (pre-heated to 70 °C) and immediately analysed. The instrument was set to 30 °C and the plate was shaken for 10 s before analysis. To determine the pH range of vesicle formation data from multiple solutions were collated and a plot of pH versus absorbance was prepared. Minimal OD values indicate the presence of micelles. As the SCAs are gradually protonated, vesicles begin to form and the OD increases. Maximum values are obtained once SCAs become fully protonated and begin to form droplets as opposed to vesicles (Extended Data Fig. 1). To allow for better data visualisation and comparison, values in Figure 1 were normalised and fit to a sigmoid model representing the phase transition of the solutions. The initial upward turning point of the curve was defined as the transition point whereby vesicle formation begins. Interpretations made based on these plots were confirmed by confocal and electron microscopy.

CBC was also determined by OD measurement. Solutions were prepared in a range of concentrations and analysed as previously described. Data were interpreted following the same

procedure as Maurer and Nguyen⁵⁴. A linear function was fit through baseline values and through increasing values. The point of intersection of these two lines corresponds to the CBC and was determined algebraically.

Encapsulation and release of pyranine dye

Encapsulation capacity of vesicles was determined by preparation of solutions in the presence of 10 μ M pyranine dye. All solutions were maintained at 70 °C during the procedure. A 200 μ L aliquot of the solution was then separated by size exclusion chromatography using a glass column (30 x 1 cm) filled with Sephadex G-50 medium beads. Fractions (3 drops, ~130 μ L total) were collected in a Falcon black 96-well plate and analysed immediately. Encapsulation was measured by fluorescence spectroscopy on an Infinite M200 Pro spectrophotometer (Tecan) using excitation and emission wavelengths of 450 and 508 nm respectively. Data were processed using the Magellan software package. Vesicle fractions were combined and separated again by size exclusion chromatography after 24 hours to determine release of pyranine over time.

Confocal microscopy

Confocal microscopy of vesicle solutions was performed on a Zeiss LSM-T-PMT with an Ar laser at 514 nm coupled to an Airyscan detector. 0.5 μ L of 100 μ M rhodamine-6G was added to a heated glass slide followed by 5 μ L of sample solution. These were mixed on the slide and covered with a heated coverslip. Images were captured using a 63X oil objective.

Negative-staining Transmission Electron Microscopy (NS-TEM)

Samples were analysed by TEM using a negative staining (NS-TEM) method. A drop of sample solution was applied to a copper TEM grid and allowed to stand for 1 minute. Excess sample was removed by blotting with filter paper. An aliquot of 1.5% aqueous uranyl acetate solution was

applied to the grid for a further 1 minute and the excess was subsequently removed with filter paper. Samples were analysed immediately on a JEOL 1010 TEM (JEOL, Japan).

Cryogenic TEM

Samples were applied directly to glow-discharged Lacey Carbon (400 mesh Cu) grids (Agar Scientific) for 30 s, blotted for 8.5 or 11 s at 4.5 °C and 95% humidity, and then rapidly plunged into liquid ethane using a Vitrobot Mark IV (Thermo Fisher). Imaging was completed using a T10 microscope (FEI) operated at 100 kV. Images were collected at a magnification range of 7000-34000x.

Data availability

All data are available in the main text, Extended Data Figs. 1-10 and Supplementary Information (Supplementary Materials and Methods, Supplementary Figs. 1-14 and Supplementary Tables 1-2.

Competing interests statement

The authors declare no competing interests.

Acknowledgements

We thank Mark Turmaine for assistance with NS-TEM, and Prof Beppe Battaglia, Prof Finn Werner and Prof Don Braben for valuable discussions. We would like to thank the anonymous reviewers whose input significantly improved the manuscript. We are grateful to the BBSRC (HR, LiDo Doctoral Training Programme) and bgc3 for funding. A.M.H and A.M. are funded by the Medical Research Council U.K. (Career Development Award MR/M00936X/1 to A.M.).

Author contributions

413 NL supervised the work; SFJ, HR, INZ, AMH, AM and NL conceived and designed the experiments;
414 SFJ, HR, INZ & AMH performed the experiments; SFJ, INZ, AMH & AM contributed materials and
415 analysis tools; SFJ & NL analysed the data; SFJ and NL wrote the paper.

416

417 **References**

- 418 Mitchell, P. in *Proceedings of the first International Symposium on the Origin of Life on the Earth,*
419 *held at Moscow, 19-24 August 1957 (I.U.B. symposium series)* 437–443 (1959).
- 420 Nitschke, W. & Russell, M. J. Hydrothermal focusing of chemical and chemiosmotic energy,
421 supported by delivery of catalytic Fe, Ni, Mo/W, Co, S and Se, forced life to emerge. *J. Mol.*
422 *Evol.* **69**, 481–496 (2009).
- 423 Fuchs, G. Alternative pathways of carbon dioxide fixation: Insights into the early evolution of
424 life? *Annu. Rev. Microbiol.* **65**, 631–658 (2011).
- 425 Lane, N. & Martin, W. F. The origin of membrane bioenergetics. *Cell* **151**, 1406–1416 (2012).
- 426 Mulkidjanian, A. Y., Galperin, M. Y. & Koonin, E. V. Co-evolution of primordial membranes and
427 membrane proteins. **34**, 206–215 (2009).
- 428 Koga, Y., Kyuragi, T., Nishihara, M. & Sone, N. Did archaeal and bacterial cells arise independently
429 from noncellular precursors? A hypothesis stating that the advent of membrane phospholipid with
430 enantiomeric glycerophosphate backbones caused the separation of the two lines of descent. *J. Mol.*
431 *Evol.* **46**, 54–63 (1998).
- 432 Martin, W. & Russell, M. J. On the origins of cells: a hypothesis for the evolutionary transitions from
433 abiotic geochemistry to chemoautotrophic prokaryotes, and from prokaryotes to nucleated
434 cells. *Philos. Trans. R. Soc. B Biol. Sci.* **358**, 59–85 (2003).
- 435 Koga, Y. Early evolution of membrane lipids: How did the lipid divide occur? *J. Mol. Evol.* **72**, 274–282
436 (2011).
- 437 Sojo, V. On the biogenic origins of homochirality. *Orig. Life Evol. Biosph.* **45**, 219–224 (2015).

438 Lombard, J., López-García, P. & Moreira, D. The early evolution of lipid membranes and the three
 439 domains of life. *Nat. Rev. Microbiol.* **10**, 507–515 (2012).
 440 Shimada, H. & Yamagishi, A. Stability of heterochiral hybrid membrane made of bacterial sn-G3P
 441 lipids and archaeal sn-G1P lipids. *ACS Biochem.* **50**, 4114–4120 (2011).
 442 Caforio, A., Siliakus, M. F., Exterkate, M., Jain, S. & Jumde, V. R. Converting *Escherichia coli* into an
 443 archaeobacterium with a hybrid heterochiral membrane. *PNAS* **115**, 3705–3709 (2018).
 444 Hanczyc, M. M. & Szostak, J. W. Replicating vesicles as models of primitive cell growth and
 445 division. *Curr. Opin. Chem. Biol.* **8**, 660–664 (2004).
 446 Chen, I. A. & Szostak, J. W. Membrane growth can generate a transmembrane pH gradient in fatty
 447 acid vesicles. *PNAS* **101**, 7965–7970 (2004).
 448 Chen, I. A. & Szostak, J. W. A kinetic study of the growth of fatty acid vesicles. *Biophys. J.* **87**, 988–
 449 998 (2004).
 450 Sojo, V., Pomiankowski, A. & Lane, N. A bioenergetic basis for membrane divergence in archaea and
 451 bacteria. *PLoS Biol.* **12**, e1001926 (2014).
 452 Segré, D., Ben-Eli, D., Deamer, D. W. & Lancet, D. The lipid world. *Orig. Life Evol. Biosph.* **31**, 119–145
 453 (2001).
 454 Segré, D., Ben-Eli, D. & Lancet, D. Compositional genomes: Prebiotic information transfer in mutually
 455 catalytic noncovalent assemblies. *PNAS* **97**, 4112–4117 (2000).
 456 Amend, J. P. & McCollom, T. M. Energetics of biomolecule synthesis on early earth. *ACS Symp.*
 457 *Ser.* **1025**, 63–94 (2009).
 458 Martin, W. Carbon-metal bonds: rare and primordial in metabolism. *Trends Biochem. Sci.* **44**, 807–
 459 818 (2019).
 460 McCollom, T. M., Ritter, G. & Simoneit, B. R. T. Lipid synthesis under hydrothermal conditions
 461 by Fischer-Tropsch reactions. *Orig. life Evol. Biosph.* **29**, 153–166 (1999).

462 Scheidler, C., Sobotta, J., Eisenreich, W., Wächtershäuser, G. & Huber, C. Unsaturated C₃,₅,₇,₉-
 463 monocarboxylic acids by aqueous, one-pot carbon fixation: possible relevance for the origin of
 464 life. *Sci. Rep.* **6**, 27595 (2016).
 465 Decker, P. & Schweer, H. Reactions in the formol bioid: the origin of branched chains of isoprenoids,
 466 valine, and leucines. *Orig. Life* **14**, 335–342 (1984).
 467 Prey, H. A., Schweickert, C. E. & Minnich, B. H. Solubility of hydrogen, oxygen, nitrogen, and helium
 468 in water. *Ind. Eng. Chem.* **44**, 1146–1151 (1952).
 469 Baaske, P. *et al.* Extreme accumulation of nucleotides in simulated hydrothermal pore systems. *Proc.*
 470 *Natl. Acad. Sci.* **104**, 9346–9351 (2007).
 471 Budin, I., Bruckner, R. J. & Szostak, J. W. Formation of protocell-like vesicles in a thermal diffusion
 472 column. *J.A.C.S Commun.* **131**, 9628–9629 (2009).
 473 Hanczyc, M. M., Mansy, S. S. & Szostak, J. W. Mineral surface directed membrane assembly. *Orig.*
 474 *Life Evol. Biosph.* **37**, 67–82 (2007).
 475 Buckel, W. & Thauer, R. K. Flavin-based electron bifurcation, ferredoxin, flavodoxin, and anaerobic
 476 respiration with protons (Ech) or NAD⁺ (Rnf) as electron acceptors: a historical review. *Front.*
 477 *Microbiol.* **9**, 401 (2018).
 478 West, T., Sojo, V., Pomiankowski, A. & Lane, N. The origin of heredity in protocells. *Philos. Trans. R.*
 479 *Soc. B Biol. Sci.* **372**, 20160419 (2017).
 480 Russell, M. J. & Hall, A. J. The emergence of life from iron monosulphide bubbles at a submarine
 481 hydrothermal redox and pH front. *J. Geol. Soc. London.* **154**, 377–402 (1997).
 482 Russell, M. J. & Martin, W. The rocky roots of the acetyl-CoA pathway. *Trends Biochem. Sci.* **29**, 358–
 483 363 (2004).
 484 Russell, M. J., Daniel, R. M., Hall, A. J. & Sherringham, J. A hydrothermally precipitated catalytic iron
 485 sulphide membrane as a first step toward life. *J. Mol. Evol.* **39**, 231–243 (1994).
 486 Martin, W. & Russell, M. J. On the origin of biochemistry at an alkaline hydrothermal vent. *Philos.*
 487 *Trans. R. Soc. Lond. B. Biol. Sci.* **362**, 1887–1925 (2007).

488 Martin, W., Baross, J., Kelley, D. & Russell, M. J. Hydrothermal vents and the origin of life. *Nat. Rev.*
 489 *Microbiol.* **6**, 805–814 (2008).
 490 Russell, M. J. *et al.* The drive to life on wet and icy worlds. *Astrobiology* **14**, 308–343 (2014).
 491 Monnard, P.-A., Apel, C. L., Kanavarioti, A. & Deamer, D. W. Influence of ionic inorganic solutes on
 492 self-assembly and polymerization processes related to early forms of life: implications for a prebiotic
 493 aqueous medium. *Astrobiology* **2**, 139–152 (2002).
 494 Monnard, P. A. & Deamer, D. W. Membrane self-assembly processes: Steps toward the first cellular
 495 life. *Anat. Rec.* **207**, 123–151 (2002).
 496 Szostak, J. W., Bartel, D. P. & Luisi, P. L. Synthesizing life. *Nature* **409**, 387–390 (2001).
 497 Deamer, D. The role of lipid membranes in life's origin. *Life* **7**, 5 (2017).
 498 Milshteyn, D, Damer, B., Havig, J. & Deamer, D. Amphiphilic compounds assemble into membranous
 499 vesicles in hydrothermal hot spring water but not in seawater. *Life* **8**, 11 (2018).
 500 Maurer, S. The impact of salts on single chain amphiphile membranes and implications for the
 501 location of the origin of life. *Life* **7**, 44 (2017).
 502 Maurer, S. E. *et al.* Vesicle self-assembly of monoalkyl amphiphiles under the effects of high ionic
 503 strength, extreme pH, and high temperature environments. *Langmuir* **34**, 15560–68 (2018).
 504 Apel, C. L., Deamer, D. W. & Mautner, M. N. Self-assembled vesicles of monocarboxylic acids and
 505 alcohols: conditions for stability and for the encapsulation of biopolymers. *Biochim. Biophys. Acta*
 506 **1519**, 1–9 (2002).
 507 Rendón, A., Gil Carton, D., Sot, J., García-Palacios, M., Montes, R., Valle, M., Arrondo, J-L. R., Goñi,
 508 F.M. & Ruiz-Mirazo, K. Model systems of precursor cellular membranes: long-chain alcohols stabilize
 509 spontaneously formed oleic acid vesicles. *Biophys. J.* **102**, 278–286 (2012).
 510 Namani, T. & Deamer, D. W. Stability of model membranes in extreme environments. *Orig. Life Evol.*
 511 *Biosph.* **38**, 329–341 (2008).

512 Cape, J. L., Monnard, P. A. & Boncella, J. M. Prebiotically relevant mixed fatty acid vesicles support
 513 anionic solute encapsulation and photochemically catalyzed trans-membrane charge transport.
 514 *Chem. Sci.* **2**, 661–671 (2011).

515 Monnard, P. A. & Deamer, D. W. Preparation of vesicles from nonphospholipid amphiphiles.
 516 *Methods Enzymol.* **372**, 133–151 (2003).

517 Thanh Thuy, D., Decnop-Weever, D., Th. Kok, W., Luan, P. & Vong Nghi, T. Determination of traces of
 518 calcium and magnesium in rare earth oxides by flow-injection analysis. *Anal. Chim. Acta* **295**, 151–
 519 157 (1994).

520 Avnir, Y. & Barenholz, Y. pH determination by pyranine: medium-related artifacts and their
 521 correction. *Anal. Biochem.* **347**, 34–41 (2005).

522 Kelley, D. S. *et al.* An off-axis hydrothermal vent field near the Mid-Atlantic Ridge at 30 degrees
 523 N. *Nature* **412**, 145–149. (2001).

524 Kelley, D. S. *et al.* A serpentinite-hosted ecosystem: The Lost City hydrothermal
 525 field. *Science* **307**, 1428–1434 (2005).

526 Smith, R. & Tanford, C. Hydrophobicity of long chain n-alkyl carboxylic acids, as measured by their
 527 distribution between heptane and aqueous solutions. *PNAS* **70**, 289–293 (1973).

528 Budin, I., Prywes, N., Zhang, N. & Szostak, J. W. Chain-length heterogeneity allows for the assembly
 529 of fatty acid vesicles in dilute solution. *Biophys. J.* **107**, 1582–90 (2014).

530 Maurer, S. E. & Nguyen, G. Prebiotic vesicle formation and the necessity of salts. *Orig. Life Evol.*
 531 *Biosph.* **46**, 215–222 (2016).

532 Hargreaves, W. R. & Deamer, D. W. Liposomes from ionic, single-chain amphiphiles.
 533 *Biochemistry* **17**, 3759–3768 (1978).

534 Sojo, V., Herschy, B., Whicher, A., Camprubí, E. & Lane, N. The origin of life in alkaline hydrothermal
 535 vents. *Astrobiology* **16**, 181–197 (2016).

536 Marty, B., Avice, G., Bekaert, D. V & Broadley, M. W. Salinity of the Archaean oceans from analysis of
 537 fluid inclusions in quartz. *Comptes rendus - Geosci.* **350**, 154–163 (2018).

538 Holland, H. D. *The Chemical Evolution of the Atmosphere and Oceans*. (Princeton University Press,
539 1984).

540 Fyfe, W. S. The water inventory of the Earth: fluids and tectonics. *Geological Soc. Spec. Publ.* **78**, 1–7
541 (1994).

542 Arndt, N. T. & Nisbet, E. G. Processes on the young earth and the habitats of early life. *Annu. Rev.*
543 *Earth Planet. Sci.* **40**, 521–549 (2012).

544 Russell, M. J. & Arndt, N. T. Geodynamic and metabolic cycles in the Hadean. *Biogeosciences* **2**, 97–
545 111 (2005).

546 Lopresti, C., Lomas, H., Massignani, M., Smart, T. & Battaglia, G. Polymersomes: nature inspired
547 nanometer sized compartments. *J. Mater. Chem.* **19**, 3576–3590 (2009).

548 Smart, T. *et al.* Block copolymer nanostructures. *Nanotoday* **3**, 38–46 (2008).

549 Bonaccio, S., Wessicken, M., Berti, D., Walde, P. & Luisi, P. L. Relation between the molecular
550 structure of phosphatidyl nucleosides and the morphology of their supramolecular and mesoscopic
551 aggregates. *Langmuir* **12**, 4976–4978 (1996).

552 Morse, J. W. & Mackenzie, F. T. Hadean ocean carbonate geochemistry. *Aquat. Geochemistry* **4**,
553 301–319 (1998).

554 Holm, N. G. The significance of Mg in prebiotic geochemistry. *Geobiology* **10**, 269–279 (2012).

555 Ludwig, K. A., Kelley, D. S., Butterfield, D. A., Nelson, B. K. & Fru-Green, G. Formation and evolution
556 of carbonate chimneys at the Lost City Hydrothermal Field. *Geochim. Cosmochim. Acta* **70**, 3625–
557 3645 (2006).

558 Adamala, K. & Szostak, J. W. Nonenzymatic template-directed RNA synthesis inside model
559 protocells. *Science* **342**, 1098–1101 (2013).

560 Jordan, S. F., Nee, E., & Lane, N. Isoprenoids enhance the stability of fatty acid membranes at the
561 emergence of life potentially leading to an early lipid divide. *Interface Focus* 20190067 (2019).

562 Camprubi, E., Jordan, S. F., Vasiliadou, R. & Lane, N. Iron catalysis at the origin of life. *IUBMB*
563 *Life* **69**, 373–381 (2017).

564 Lane, N., Allen, J. F. & Martin, W. How did LUCA make a living? Chemiosmosis in the origin of
565 life. *BioEssays* **32**, 271–280 (2010).
566 Harrison, S. & Lane, N. Life as a guide to prebiotic nucleotide synthesis. *Nat. Commun.* **9**, 5176
567 (2018).
568
569

Figure legends

Figure 1. Plots of normalised absorbance at 480 nm versus pH, with corresponding confocal micrographs for the transition point from the micellar to vesicular phase, for 50 mM C₁₀ fatty acid (a), 5 mM C₁₀-C₁₅ fatty acid mixture (b), and 5 mM 5:1 C₁₀-C₁₅ fatty acid/1-alkanol mixture (c). Error bars in (a), (b), and (c) represent the standard deviation (n = 3).

Figure 2. Plot of absorbance at 480 nm versus pH for 5 mM 1:1 C₁₀-C₁₅ fatty acid/1-alkanol mixture (a) with corresponding confocal micrographs at pH 7.09 (b), pH 10.45 (c), and pH 12.13 (d). Error bars in (a) represent the standard deviation (n = 3).

Figure 3. (a) Encapsulation of the fluorescent dye pyranine, showing a peak for pyranine encapsulated within vesicles composed of 5 mM 1:1 C₁₀-C₁₅ fatty acid/1-alkanol mixture at FN ~20, and a larger peak for free dye at FN ~70. (b) Vesicles as in (a) but after 24 h encapsulation, with ~20% of the encapsulated pyranine peak remaining at FN ~20. (c) and (d) Equivalent plots for the full 5 mM 1:1:1 C₁₀-C₁₅ fatty acid/1-alkanol/C₁₀ isoprenoid mixture. (e) Fluorescence from free pyranine in water (solid line) and water with full salt solution at pH 12 (dotted line), showing interaction of dye with salt mixture leading to a substantially lower free pyranine peak after chromatography. (f) Encapsulation of pyranine in vesicles composed of 5 mM 1:1:1 C₁₀-C₁₅ fatty acid/1-alkanol/C₁₀ isoprenoid mixture, with encapsulated pyranine fluorescence at FN ~20 and free dye at FN ~70. Note log scale on Y axis to emphasise encapsulation despite disruption from salt interactions. Pink shading in (a) and (c) represents the standard deviation (n = 3).

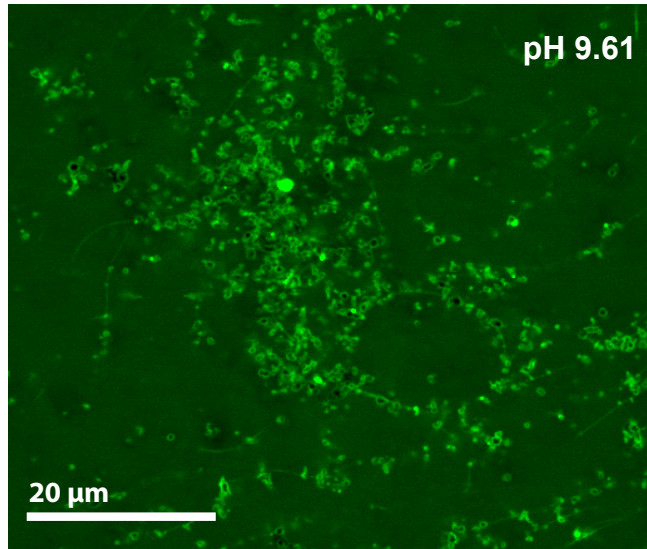
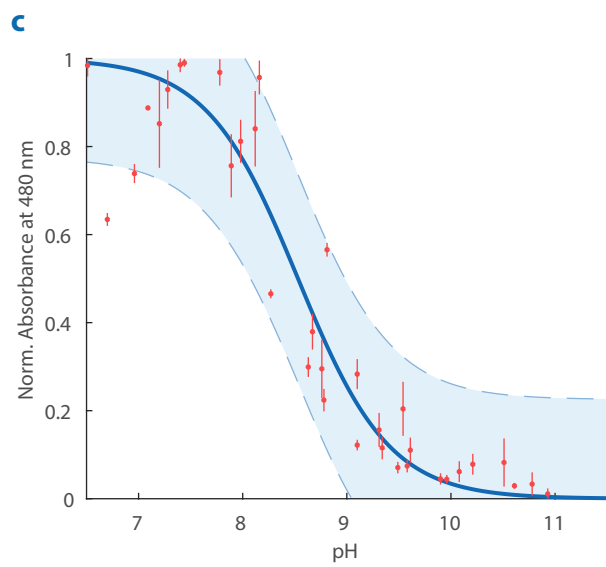
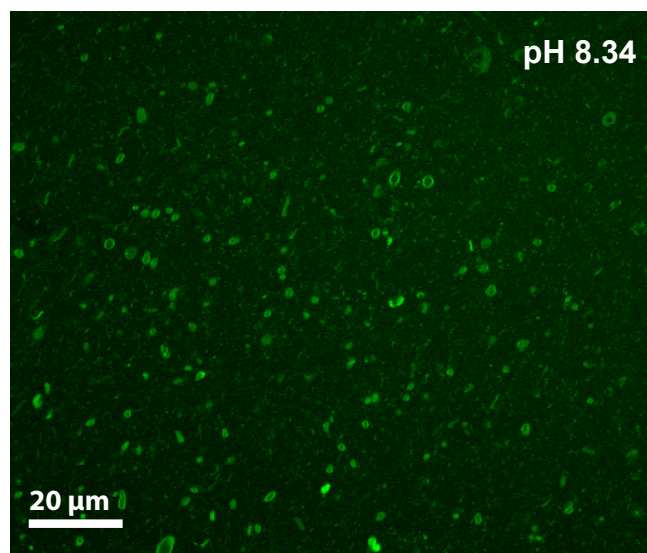
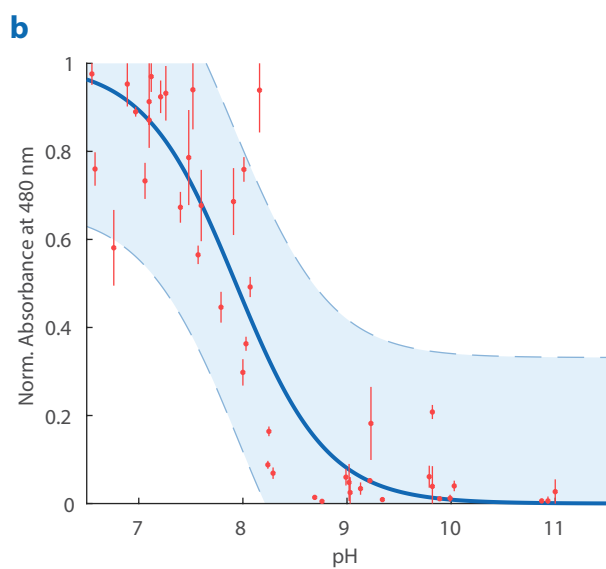
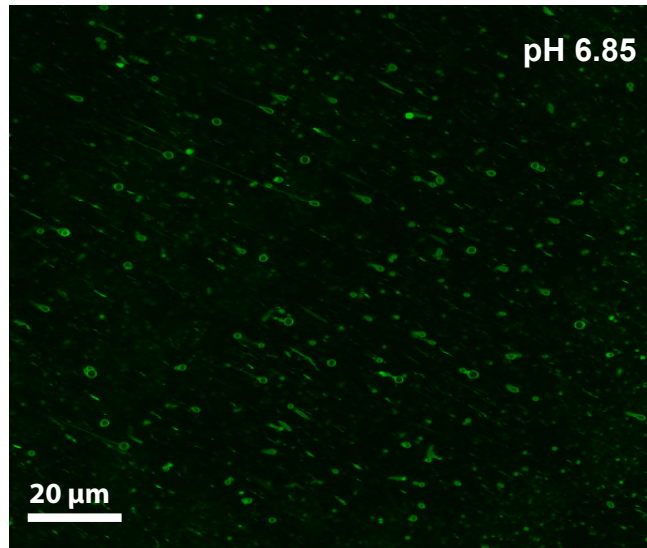
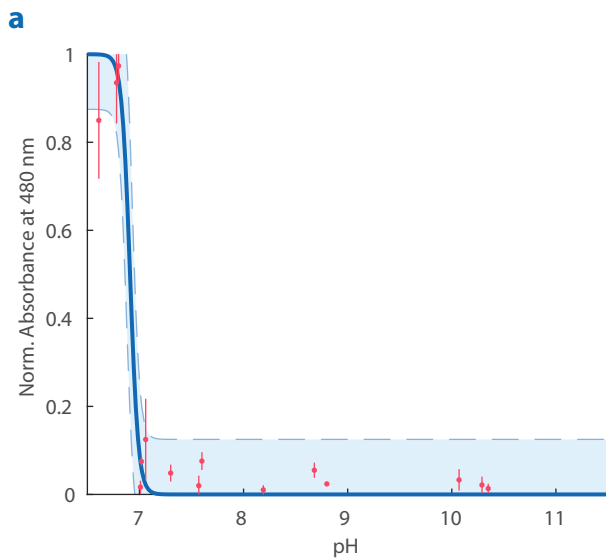
Figure 4. a Plot of absorbance at 480 nm versus concentration for C₁₀-C₁₅ fatty acid mixture at pH ~8 and C₁₀ fatty acid at pH ~7 showing calculated critical bilayer concentrations (CBC) of 1.35 mM and 39 mM respectively (with each individual FA present at 225 µM). Error bars represent the standard

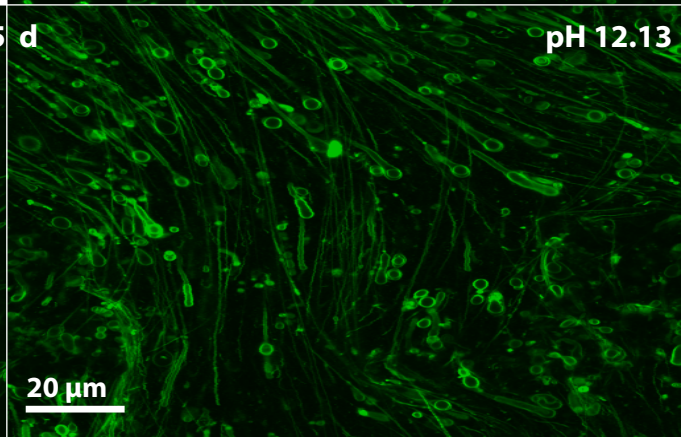
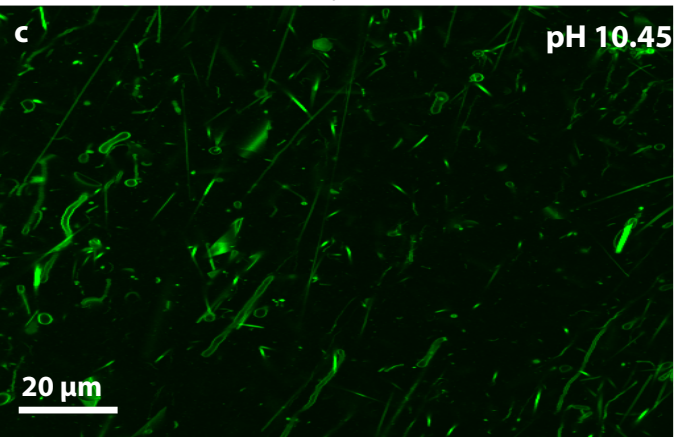
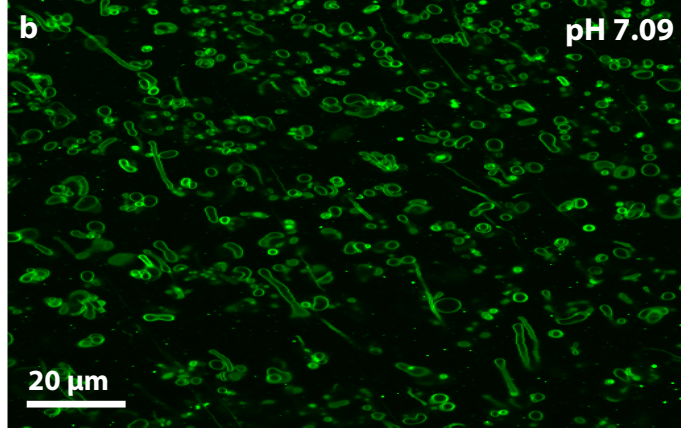
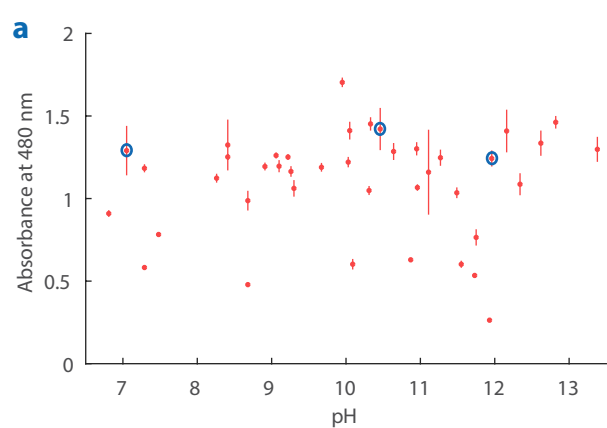
deviation ($n = 3$). **b** Cryo-TEM micrograph of 600 μM 1:1 $\text{C}_{10}\text{-C}_{15}$ fatty acid/alcohol mixture at pH 7.71 (with each individual FA present at 100 μM).

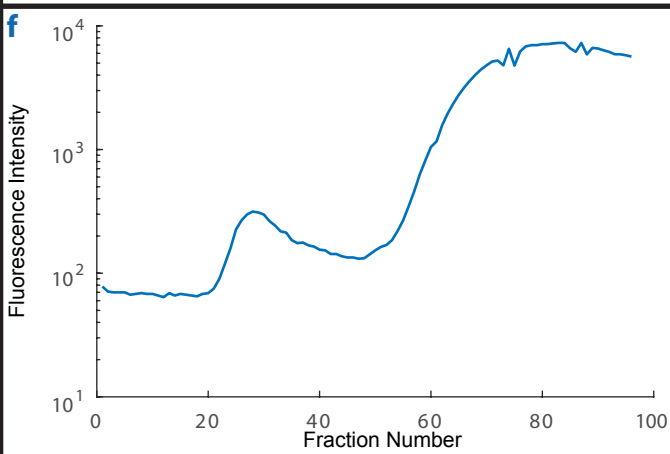
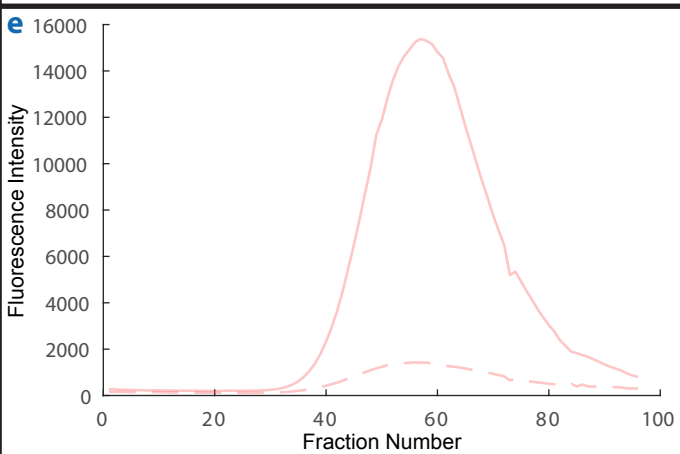
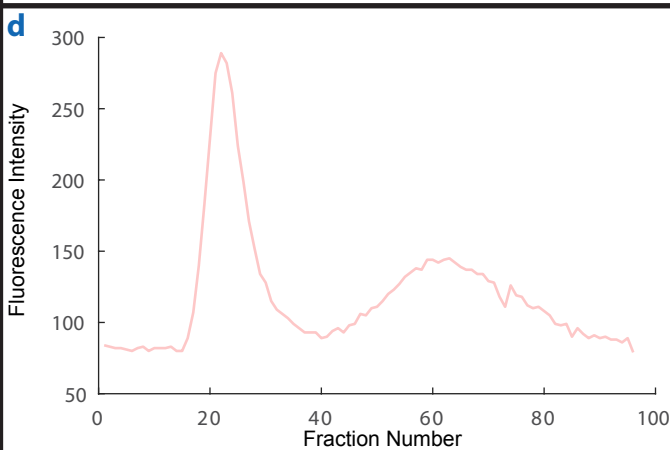
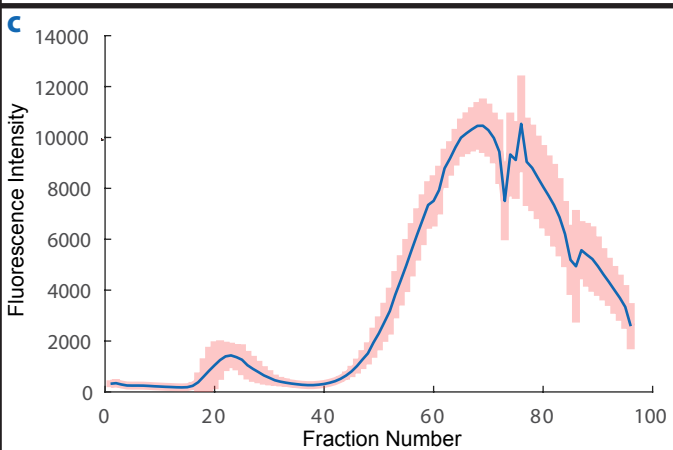
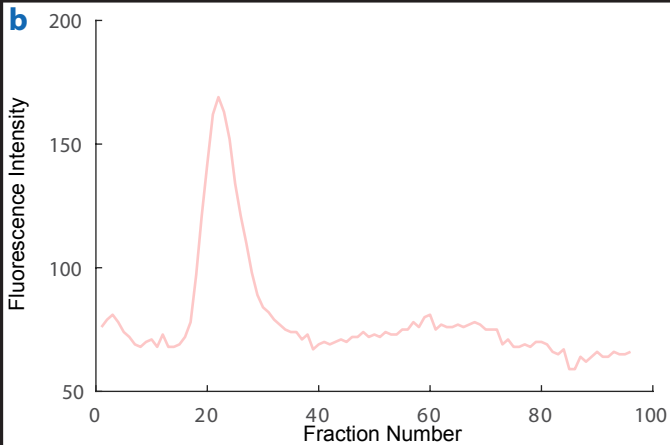
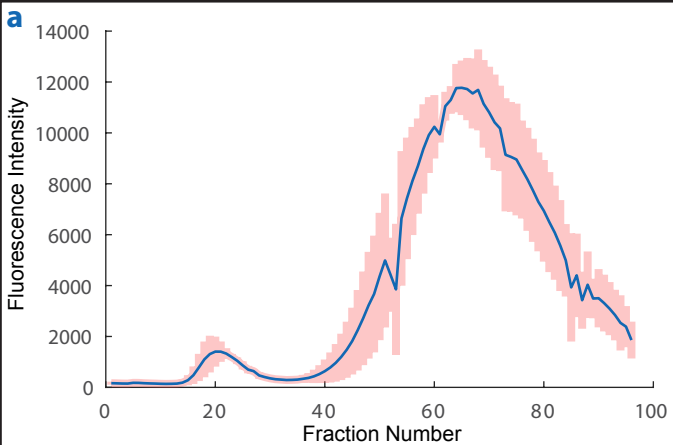
Figure 5. Confocal micrographs of 5 mM 1:1 $\text{C}_{10}\text{-C}_{15}$ fatty acid/alcohol mixture in 600 mM NaCl pH 11.17 (**a**), 50 mM MgCl_2 pH 11.65 (**b**), and 10 mM CaCl_2 pH 11.84 (**c**) along with corresponding Cryo-TEM micrographs at pH 12.17 (**d**), pH 12.31 (**e**), and pH 12.29 (**f**).

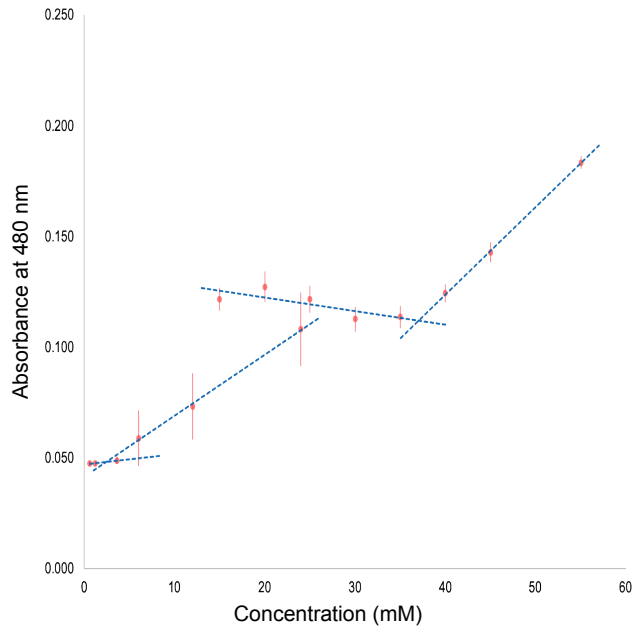
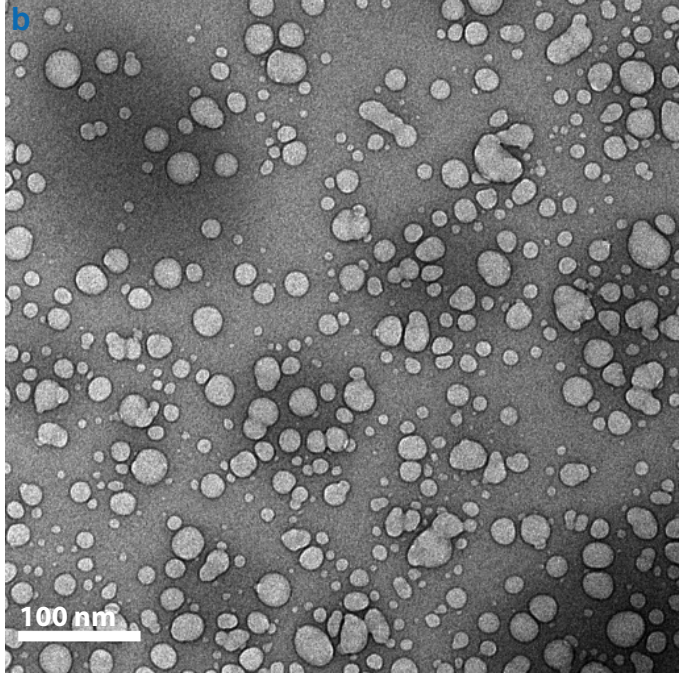
Figure 6. Filamentous vesicle aggregates formed in a solution of 5 mM $\text{C}_{10}\text{-C}_{15}$ fatty acids in 100 mM NaCl as observed by confocal microscopy (**a**) and NS-TEM (**b**, **c**, and **d**). During NS-TEM, vesicles burst under vacuum leading to collapsed structures as seen in these micrographs.

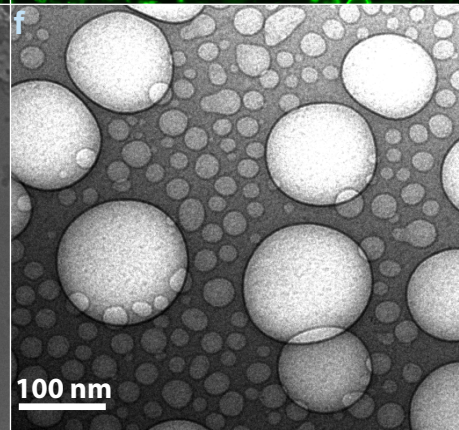
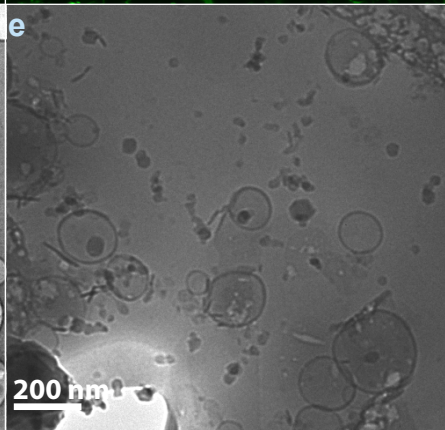
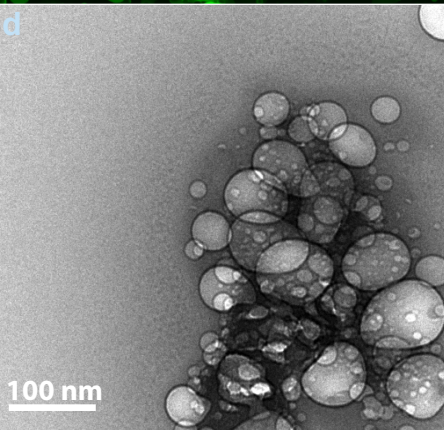
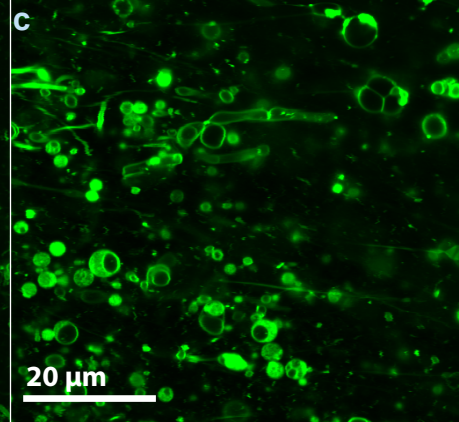
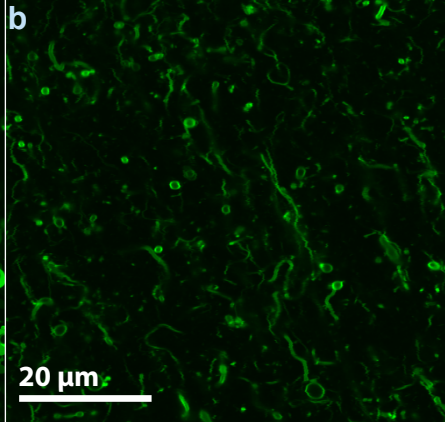
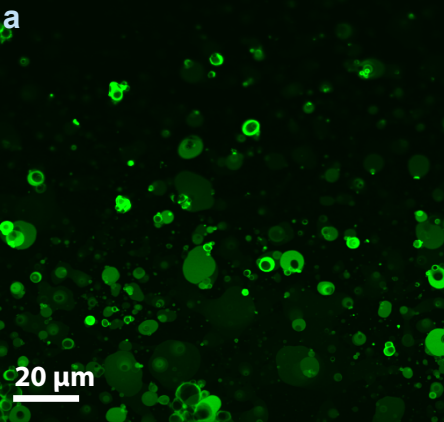
Figure 7. Confocal (**a**) and Cryo-TEM (**b**) micrographs of 5 mM 1:1:1 $\text{C}_{10}\text{-C}_{15}$ fatty acid/alcohol/ C_{10} isoprenoid mixture in a combined solution of 600 mM NaCl, 50 mM MgCl_2 , and 10 mM CaCl_2 at pH 12.69 and 11.75 respectively.

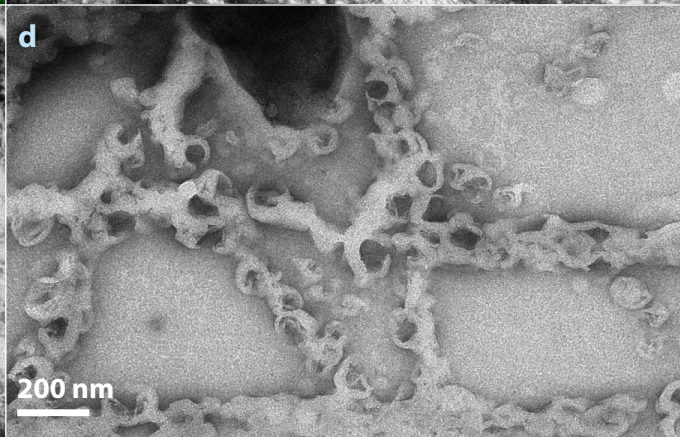
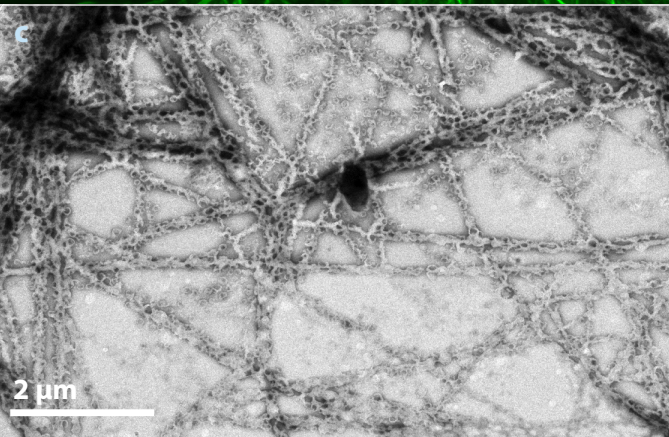
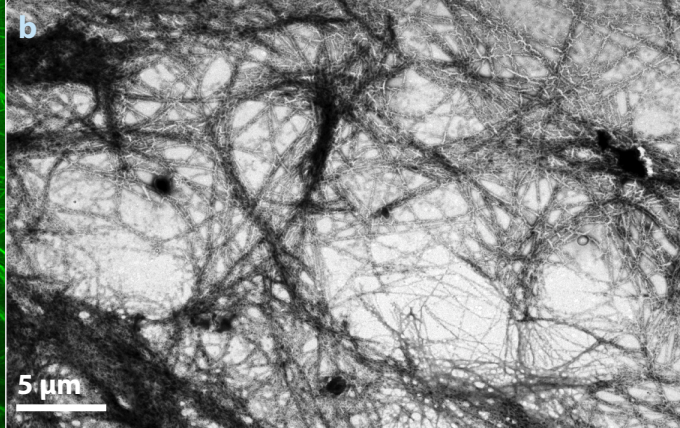
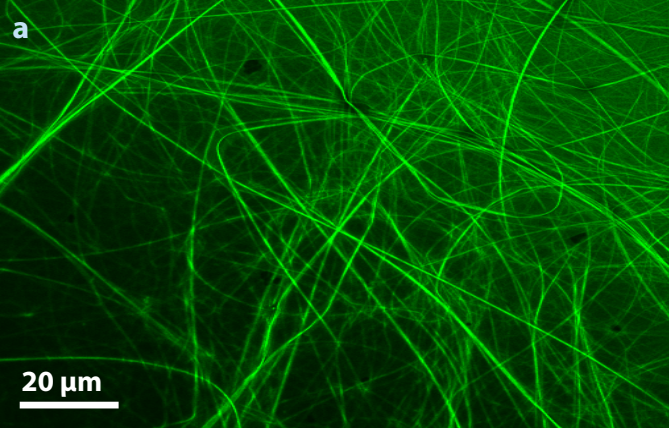


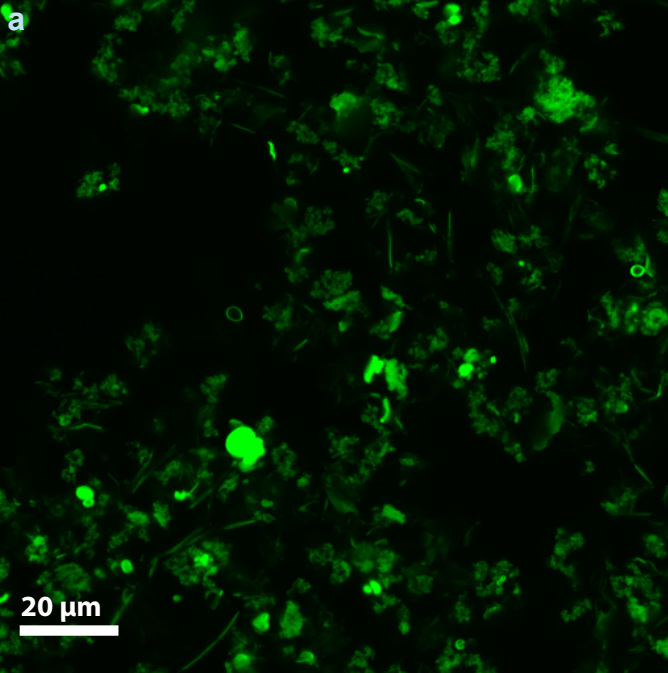
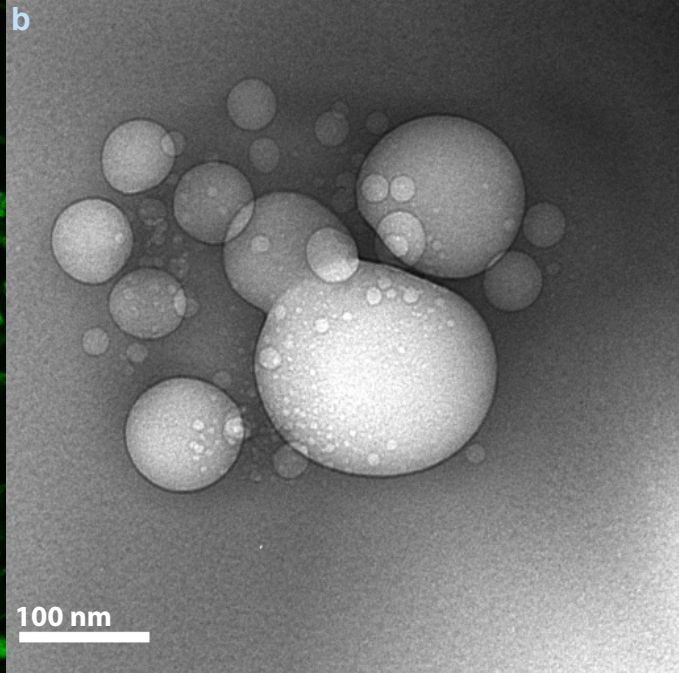




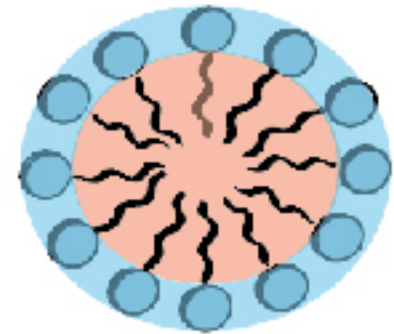
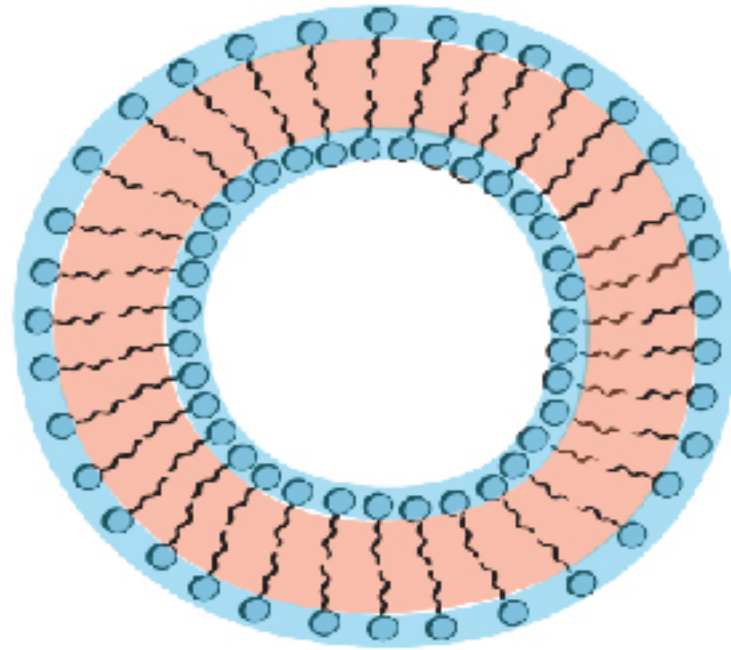
a**b**





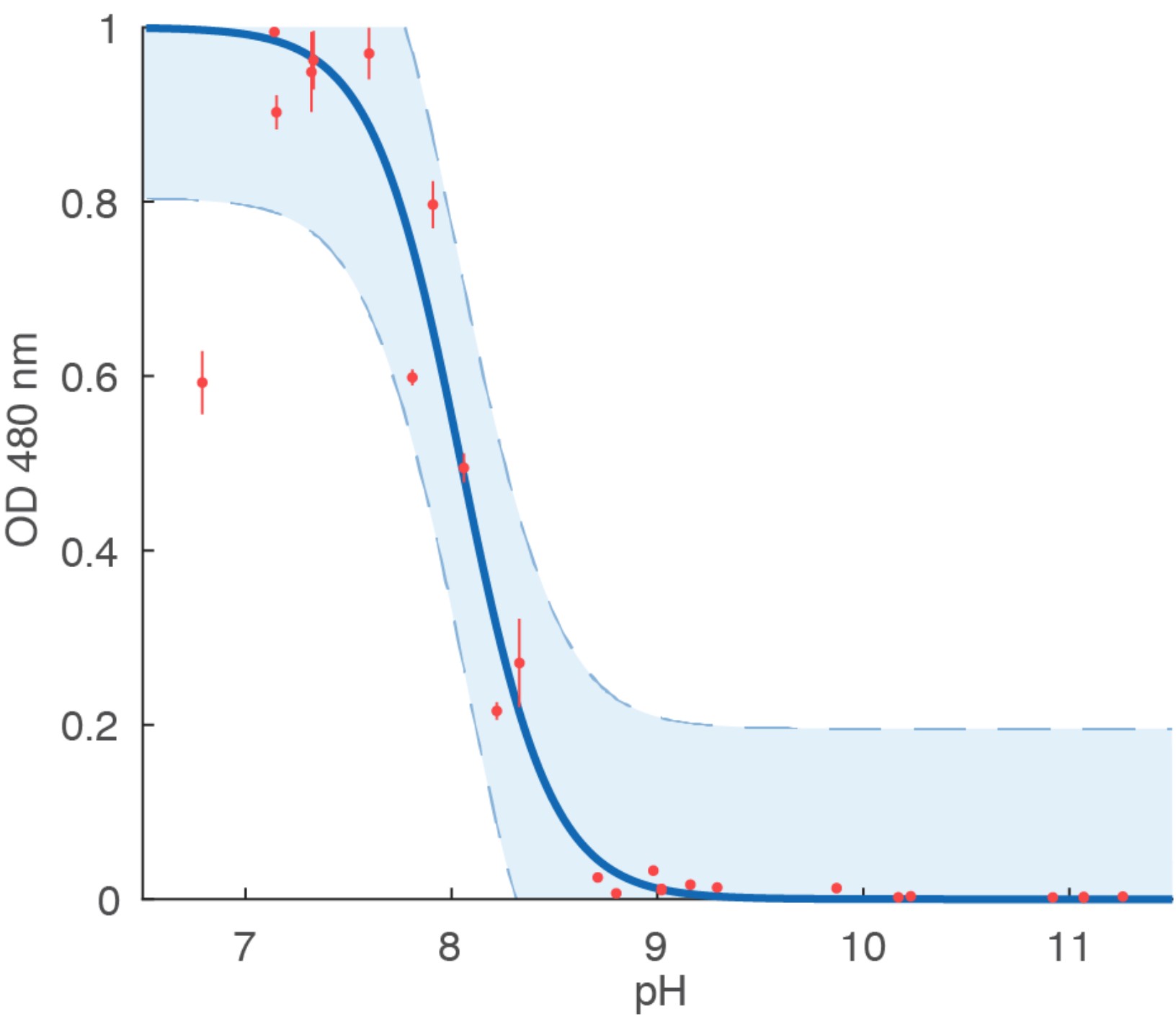
a**b**

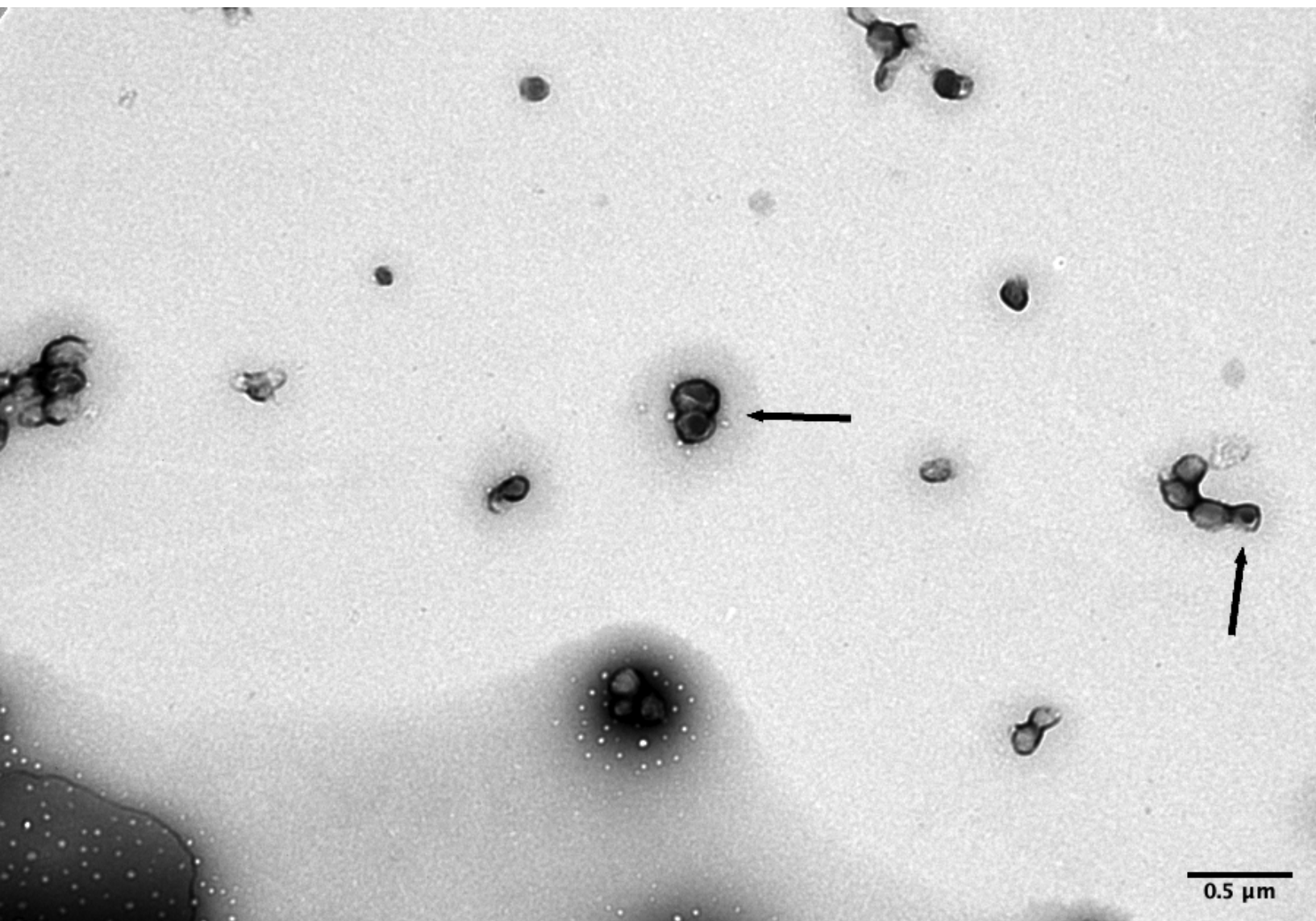
Droplet ← Vesicle ← Micelle

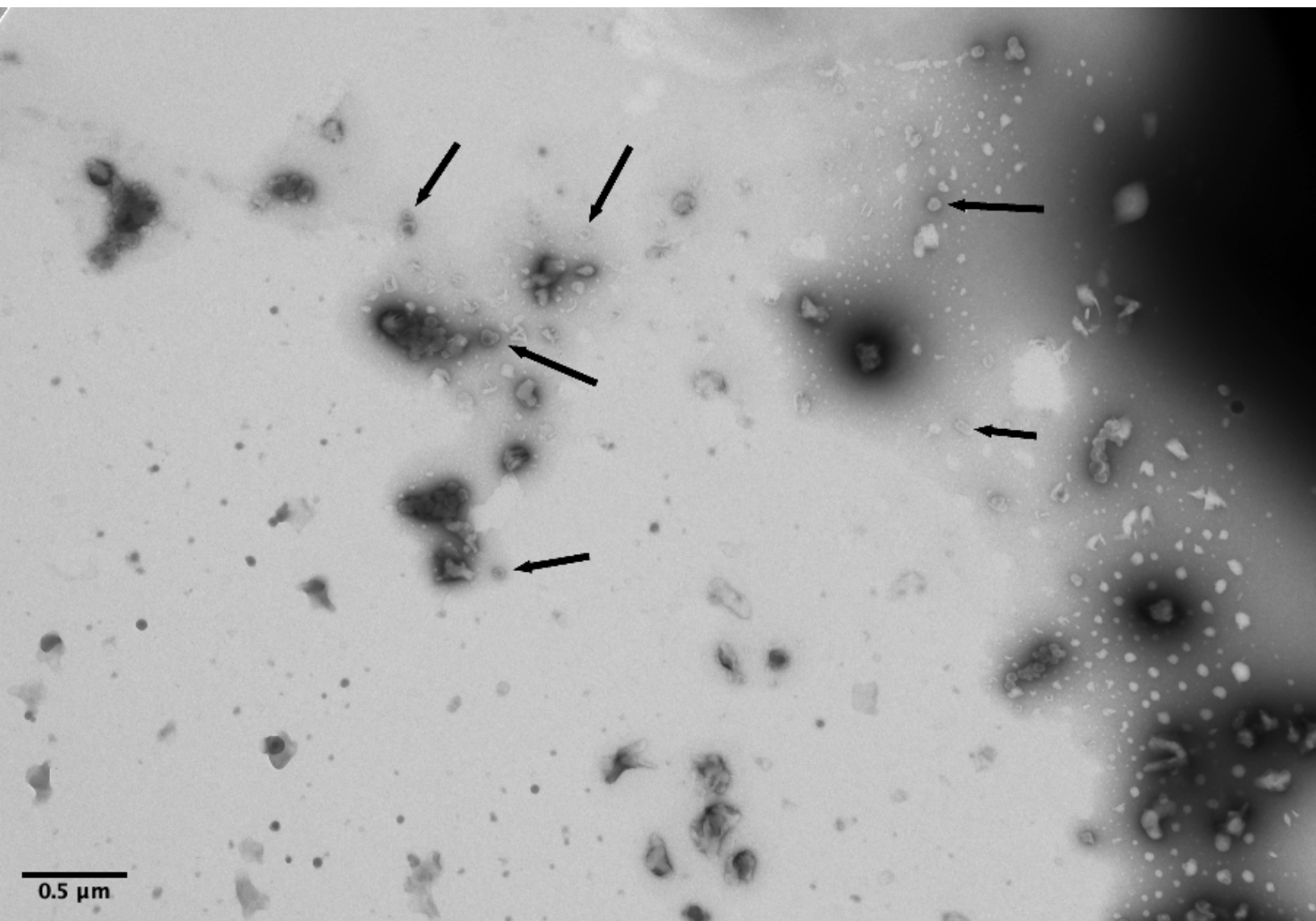


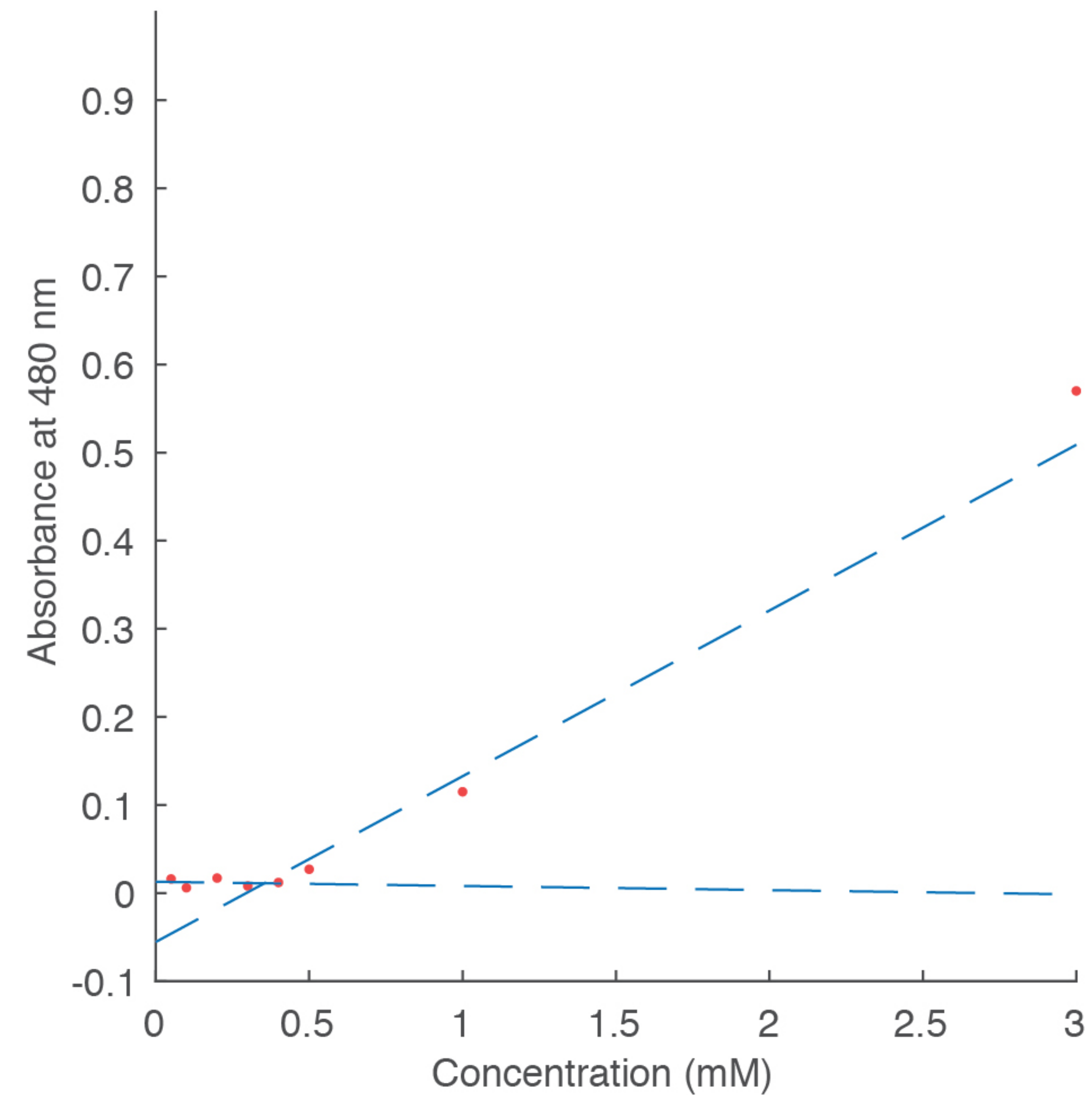
pH









a**b**